RSC Sustainability

ROYAL SOCIETY OF CHEMISTRY

PAPER

View Article Online
View Journal | View Issue

Check for updates

Cite this: *RSC Sustainability*, 2025, **3**, 4108

Selective ring-opening of furfuryl alcohol to 1,5-pentanediol over Pt/aluminosilicates†

Lee J. Durndell, *[a] Vannia C. dos Santos-Durndell, [a] Atal Shivhare, [b] James A. Hunns,[c] Karen Wilson *[d] and Adam F. Lee *[d]

Biomass-derived diols are key chemical building blocks for the sustainable chemical manufacturing of textiles and plastics, however their synthesis by a selective, scalable process from holocellulose is challenging. Furfuryl alcohol (FALC) is a potential precursor to 1,5-pentanediol (1,5-PeD) through acid-catalysed hydrogenolysis, and hence the impact of oxide support acidity on this reaction over Pt nanoparticles was investigated under batch and continuous flow in toluene. Platinum dispersed over weakly acidic fumed silica and mesoporous SBA-15 supports was almost inactive towards furfuryl alcohol at 150 °C and 10 bar H_2 and promoted decarbonylation and hydrodeoxygenation of FALC to furan and methyltetrahydrofuran, respectively. The introduction of Al^{3+} into silica supports, to form either an amorphous silica-aluminate (ASA) or mesoporous Al-SBA-15, selectively activated the cyclic ether bond at the C2–O position, increasing the specific activity for FALC conversion in continuous flow from 20 mmol g_{Pt}^{-1} h^{-1} (Pt/SBA-15) to 295 mmol g_{Pt}^{-1} h^{-1} (Pt/ASA), and 1,5-PeD selectivity from ~25% (Pt/SBA-15) to 65% (Pt/ASA). This synergy between metal and acid sites resulted in a >25-fold enhancement in 1,5-PeD productivity, reaching 186 mmol g_{Pt}^{-1} h^{-1} for Pt/ASA, and was maintained for 7 h time-on-stream with negligible deactivation or metal leaching. A moderately acidic Pt/γ-Al_2O_3 catalyst exhibited reactivity intermediate between that of the Pt/silica and Pt/aluminosilicate catalysts. The yield of 1,5-PeD was directly proportional to the support acid site loading, indicating a common reaction mechanism. These findings demonstrate the striking promotion of metal catalysed hydrogenation that can be achieved through judicious support selection, and its translation from batch to flow with similar reaction kinetics.

Received 26th April 2025
Accepted 14th July 2025

DOI: 10.1039/d5su00302d

rsc.li/rscsus

Open Access Article. Published on 15 July 2025. Downloaded on 2/3/2026 9:11:44 PM.
This article is licensed under a Creative Commons Attribution-NonCommercial 3.0 Unported Licence.

Sustainability spotlight

Efficient routes to large-scale chemical intermediates and commodity chemicals from renewable feedstocks are essential for sustainable chemical manufacturing, with 'drop in' chemicals required as direct replacements of crude oil derived feedstocks. Polyesters account for over half of synthetic fibres, with polyurethane foams, elastomers and coatings requiring αω-diol precursors. Selective hydrogenolysis of furfuryl alcohol (FALC) offers a synthesis route to bioderived 1,5-pentanediol (1,5-PeD) for such applications, but requires more atom- and energy efficient catalysts and scalable processes. Here we exploit the strong metal–acid synergy in Pt/aluminosilicate catalysts for the selective ring-opening of FALC to 1,5-PeD in continuous flow. This work aligns with the UN Sustainable Development Goals 12 – Responsible consumption and production and 9 – Industry, Innovation and Infrastructure.

Introduction

The global population is predicted to exceed 8.5 billion by 2030,[1] imposing an increasing strain on planetary resources and resulting pollution of ecosystems.[2] Decarbonisation of energy and manufacturing sectors is critical to mitigating these negative impacts, with the development of renewable energy platforms (notably solar and wind) and utilisation of sustainable carbon sourced from biomass promising technological solutions. Significant progress has been made on both fronts, with a range of platform chemicals obtainable from biomass identified to replace those traditionally derived from the petrochemical industry. Holocellulose is the most abundant form of biomass on Earth, and a primary source of such bioderived platform chemicals, which notably include furfural (from the solvothermal processing and acid dehydration of arabinose and xylose components of hemicellulose[3–6]) and its hydrogenation product, furfuryl alcohol (FALC). FALC can be converted to

[a]*School of Geography, Earth and Environmental Sciences, University of Plymouth, Plymouth PL4 8AA, UK. E-mail: lee.durndell@plymouth.ac.uk*

[b]*Department of Chemistry, Indian Institute of Technology Ropar, Rupnagar 140001, India*

[c]*European Bioenergy Research Institute, Aston University, Birmingham, B4 7ET, UK*

[d]*Centre for Catalysis and Clean Energy, School of Environment and Science, Griffith University, QLD 4222, Australia. E-mail: karen.wilson6@griffith.edu.au; adam.lee@griffith.edu.au*

† Electronic supplementary information (ESI) available. See DOI: https://doi.org/10.1039/d5su00302d

© 2025 The Author(s). Published by the Royal Society of Chemistry

Open Access Article. Published on 15 July 2025. Downloaded on 2/3/2026 9:11:44 PM.
This article is licensed under a Creative Commons Attribution-NonCommercial 3.0 Unported Licence.

value-added chemicals including 1,2-pentanediol (1,2-PeD),[7] 1,5-pentanediol (1,5-PeD),[8] tetrahydrofurfuryl alcohol (THFA),[9] 2-methyltetrahydrofuran (MTHF)[10] and furan[11] through selective hydrogenolysis, hydrogenation, or two-step dehydrogenation–decarbonylation (Scheme 1).[12]

Catalytic ring-opening of furfural and FALC to oxygenates (partial hydrogenolysis) was recently reviewed by Tomishige and co-workers.[13] Ring-opening of FALC to 1,5-PeD, through C–O bond hydrogenolysis within the furan ring, is of particular interest, due to the use of diols as building blocks for polyurethane, polyester, and plasticiser production.[14] Worldwide consumption of 1,5-PeD is ~3000 tons per year, but with a current global market value of ~US $40 million due to the limited abundance and hence high cost of C_5 petrochemical feedstocks and conversion technologies.[15] An alternative, high yielding, atom- and energy efficient route to 1,5-PeD from biomass would greatly promote its use in bioderived polymers as an alternative to other α,ω-diols (*e.g.* 1,6-hexanediol and 1,4-butanediol whose production scales and market values are at least an order of magnitude larger).[14]

FALC hydrogenolysis to a mix of 30% 1,5-PeD and 40% 1,2-PeD was first reported using a large excess of a $CuCr_2O_4$ catalyst at 175 °C and 100–150 bar H_2.[16] One-pot conversion of furfural to 1,5-PeD with a significant yield (35%) was subsequently reported using Pt/Co_2AlO_4 at 15 bar H_2 and 140 °C after 24 h,[17] and proposed to occur by rapid hydrogenation of the alcohol and subsequent slow hydrogenolysis of the ring in competition with ring hydrogenation/alcohol dehydration. Furfural conversion to 1,5-PeD with 71% yield was obtained over Pd/Ir–ReOx/SiO_2.[18] Low temperature (40 °C) hydrogenation over Pd–ReO_x sites was relatively rapid, followed by much slower, high-temperature (100 °C) hydrogenolysis over IrReO_x sites. 1,5-PeD formation being dictated by the temperature dependence of competing FALC hydrogenation (to THFA) and decarbonylation (to furan) reactions with the desired ring-opening pathway.[19–22] Higher temperatures favour 1,5-PeD[21] over Rh/SiO_2 and furan over Ru/SiO_2 (ref. 22) at the expense of THFA.

Non-precious metals show promise for the selective production of 1,5-PeD from FALC. Hydrotalcite-derived

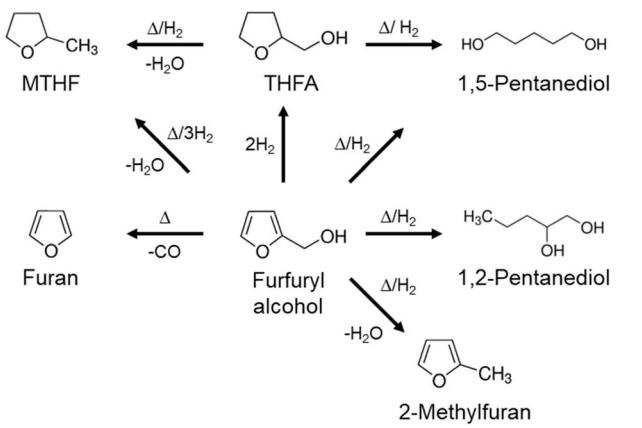

Scheme 1 Major reaction pathways for furfuryl alcohol hydrogenation/hydrogenolysis.

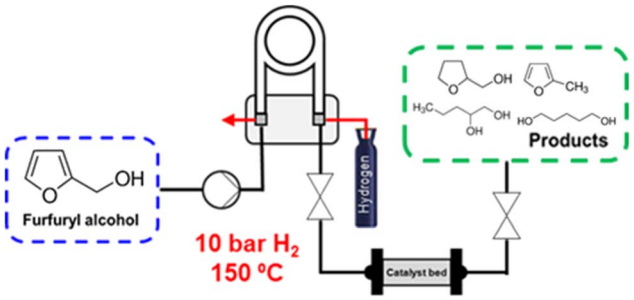

Scheme 2 Schematic of Flowsyn continuous flow reactor for the liquid phase catalytic hydrogenation of FALC to 1,5-PeD in toluene.

$Ni_1Co_{11}AlO_x$ achieved a 43% yield of 1,5-pentanediol at 160 °C and 40 bar H_2, albeit in parallel with the production of the 30% tetrahydrofurfuryl alcohol by-product.[23] An analogous $CuCoAlO_x$ catalyst gave 45% 1,5-PeD, 15% 1,2-PeD, and 22% tetrahydrofurfuryl alcohol at 140 °C, and 40 bar H_2 within 2 h,[24] and $CoMgAlO_x$ afforded 52% 1,5-PeD at 170 °C and 50 bar H_2 in 3 h.[25] Cu-doped moderately acidic H-ZSM-5 zeolites have demonstrated the highest reported yield of 1,5-PeD from FALC (84%), exploiting a continuous flow, liquid phase, fixed-bed reactor at 180 °C and 25 bar H_2 with negligible deactivation over 50 h time-on-stream, albeit with a dilute (2 wt%) FALC in ethanol feed.[26,27] A bimetallic NiSn/Al_2O_3 catalyst also achieved a promising 1,5-PeD yield of 38% in a continuous flow, vapour phase, fixed-bed reactor,[28] but required more forcing conditions of 250 °C and 40 bar H_2, and co-produced an equivalent yield of 1,2-PeD. Platinum catalysts typically exhibit poor selectivity to 1,5-PeD, with the best reported 2 wt% Pt/γ-Al_2O_3 only achieving a 15% yield at 160 °C and 10 bar H_2 in 8 h.[29] A strong synergy between metal sites, active for the dissociation of molecular hydrogen, and acid sites active for C–O bond cleavage, is important to maximise 1,5-PeD production. Inducing and optimising the metal–acid synergy[30–34] and/or the process conditions (such as substrate/catalyst contact time)[20,35,36] are strategies to improve the selectivity and yield of 1,5-PeD.

Here, we investigate the impact of support acidity on the selective conversion of FALC to diols (notably 1,5-PeD) over Pt nanoparticles in batch and continuous flow. High loadings of Brønsted and Lewis acid sites, arising from Al^{3+} species incorporated as either an ordered, mesoporous Al-SBA-15 or an amorphous silica-alumina, activate FALC for hydrogenolysis pathways over co-located Pt nanoparticles, dramatically increasing both FALC conversion and selectivity to 1,5-PeD under moderate conditions of 150 °C, 10 bar H_2. Similar reaction kinetics were obtained in batch and continuous flow operation using a packed bed Flowsyn microreactor with a GAM II coil-in-coil gas pre-saturator (Scheme 2)[37] with the added advantages of on-stream catalyst/product separation and flexible productivity.

Results and discussion

Catalyst characterisation

A family of bifunctional catalysts comprising Pt nanoparticles (~5 wt%) on fumed silica (Pt/SiO_2), SBA-15 (Pt/SBA-15), γ-

Open Access Article. Published on 15 July 2025. Downloaded on 2/3/2026 9:11:44 PM. This article is licensed under a Creative Commons Attribution-NonCommercial 3.0 Unported Licence.

alumina (Pt/γ-Al_2O_3), Al-SBA-15 (Pt/Al-SBA-15), and amorphous silica-alumina (Pt/ASA) supports was prepared by wet-impregnation with $(NH_4)_2PtCl_4$ (Table 1). Physicochemical properties of the supports and their Pt-impregnated counterparts were determined by ICP-AES, XRD, HRTEM, CO chemisorption, pyridine diffuse reflectance infrared Fourier transform spectroscopy (DRIFTS), propylamine titration, and N_2 porosimetry (Tables 1, S1, S2,† Fig. 1 and S1–S6†). The Si : Al atomic ratio was ~16 : 1 and 60 : 1 for the Al-SBA-15 and ASA supports, respectively. Silica and alumina samples, and their Pt counterparts, exhibited type II adsorption–desorption isotherms, consistent with agglomerates of non-porous primary SiO_2 or γ-Al_2O_3 particles. In contrast, all SBA-15, Al-SBA-15(15), and ASA(61) materials exhibited type IV isotherms with H1 hysteresis loops indicative of mesoporous solids with cylindrical pores in which both ends are open (Fig. S2 and S4†). Corresponding Barrett–Joyner–Halenda (BJH) pore diameters of the Pt-impregnated variants were ~5.3 ± 0.2 nm for Pt/SBA-15, 3.9 ± 0.4 nm for Pt/Al-SBA-15(15), and 3.4 ± 0.4 nm for Pt/ASA(61). Low-angle X-ray diffractograms of the parent SBA-15 and Al-SBA-15 supports showed reflections at $2\theta = 1.01°$, 1.68° and 1.91° and $2\theta = 0.94°$, 1.51°, and 1.83° respectively (Fig. S1†), assigned to the (100), (110), and (200) reflections of ordered hexagonal pore networks (Fig. S3†) with *p6mm* symmetry in accordance with literature reports,[38,39] and pore separations of 9.8 nm and 9.9 nm, respectively. These pore structures and dimensions were retained following Pt impregnation (Fig. S1, S2, S4 and S5a†). Wide angle X-ray diffractograms of Pt/silicas, Pt/γ-Al_2O_3, and Pt/aluminosilicates evidenced reflections at $2\theta = 39.9°$, 46.2°, and 67.9° characteristic of (111), (200) and (220) facets within face-centered cubic Pt metal crystallites (Fig. S5b†).[40] Corresponding volume-averaged diameters of Pt crystallites, estimated from Scherrer analysis ranged from 11.9 to 24.3 nm (Table 1), in good agreement with diameters derived from HRTEM (Fig. S6†). Note that catalysts prepared using amorphous supports (Pt/SiO_2, Pt/γ-Al_2O_3 and Pt/ASA) exhibited the expected Gaussian particle size distributions, whereas those based on ordered mesoporous supports (Pt/SBA-15 and Pt/Al-SBA-15) exhibited binomial size distributions. We attribute the latter to the formation of small Pt nanoparticles within the pores (<5 nm diameter) and larger nanoparticles on the external support surfaces (>5 nm).

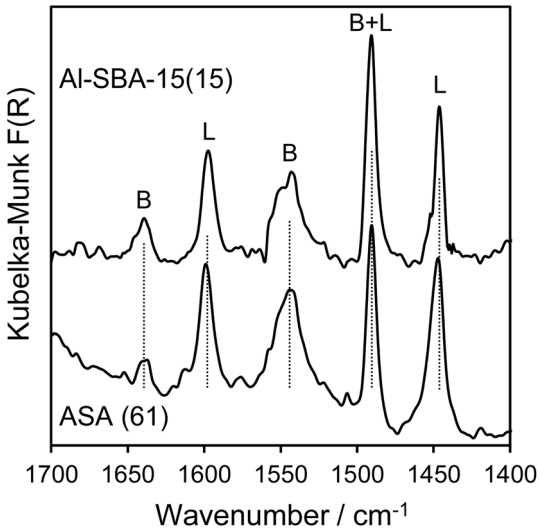

Fig. 1 *In vacuo* DRIFT spectra of chemisorbed pyridine over oxide supports; Brønsted (B) and Lewis (L) acid bands indicated.

Acidic properties of the bare oxide supports were examined by DRIFTS of pyridine (Fig. 1).[43,44] Fumed silica, SBA-15, and γ-alumina did not exhibit significant absorption bands due to Brønsted (B) acid or Lewis acid (L) bound pyridine, likely due to the low number of (weak) acid sites as previously reported.[45] In contrast, Al-SBA-15(15) and ASA(61) exhibited absorption bands at 1447 and 1597 cm^{-1} ascribed to the C=C stretches of pyridine bound to weak Lewis acid sites,[46,47] additional bands at 1548 and 1640 cm^{-1} assigned to the C=C stretching and N–H bending of protonated pyridinium cations adsorbed at Brønsted acid sites, and a band at 1492 cm^{-1} due to a pyridine adsorbed at Lewis and Brønsted acid sites.[44] A similar Brønsted : Lewis acid ratio was observed for both aluminosilicates. Zeolites possessing Lewis and/or Brønsted acidity are reported to catalyse the ring opening of furanics, and hence both are considered potential active sites in this work.[27,48–50] Total acid site loadings were quantified by propylamine titration; catalytic decomposition and the subsequent desorption temperature (300–500 °C) of reactively formed propene (m/z = 41) over acid sites provides a quantitative determination of acid strength and loading (Table S1†). Al-SBA-15(15) and ASA(61) exhibit similar acid site loadings (0.34 mmol g^{-1} and 0.37 mmol

Table 1 Structural properties of Pt/silica and Pt/aluminosilicate catalysts

Support	Pt loading[a]/wt%	Pt particle size[b]/nm	Pt dispersion[c]/%	Surface area[d]/m^2 g^{-1}	Mesopore diameter[e]/nm	Si : Al atomic ratio[a]	Acid site loading[f]/mmol g^{-1}
Fumed SiO_2	4.81	24.3 (27.0)	3.5 (±3)	146 (±15)	—	—	0.05
SBA-15	3.73	19.2 (14.9)	6.8 (±3)	569 (±57)	5.3	—	0.07
γ-Al_2O_3	4.75	11.9 (7.3)	15.4 (±3)	84 (±18)	—	—	0.11
Al-SBA-15(15)	4.97	20.9 (18.9)	4.7 (±3)	273 (±27)	3.9	14.5	0.34
ASA(61)	4.86	14.3 (9.9)	12.5 (±3)	474 (±47)	3.4	60.5	0.37

[a] ICP-AES. [b] XRD (surface-averaged HRTEM values in parentheses). [c] CO chemisorption assuming a CO : $Pt_{surface}$ stoichiometry of 0.68.[41,42] [d] BET method. [e] BJH method applied to the desorption branch. [f] TGA-MS of chemisorbed propylamine.

© 2025 The Author(s). Published by the Royal Society of Chemistry

Open Access Article. Published on 15 July 2025. Downloaded on 2/3/2026 9:11:44 PM. This article is licensed under a Creative Commons Attribution-NonCommercial 3.0 Unported Licence.

g^{-1} respectively), but respective desorption peak maxima of 441 °C and 422 °C (Fig. S7†), indicating that ASA(61) is a stronger acid[51,52] than Al-SBA-15(15).[52] In contrast, SiO_2, SBA-15 and γ-Al_2O_3 exhibited acid site loadings <0.11 mmol g^{-1}, consistent with previous reports and their weak pyridine DRIFTS, and a common propene desorption peak maximum at ~424 °C similar to that reported for SBA-15.[53] Platinum impregnation had negligible impact on the Brønsted : Lewis acid site ratios or acid loading of the parent supports, consistent with related literature.[52,54]

Furfuryl alcohol hydrogenation

Hydrogenation of FALC over the preceding Pt catalysts was investigated in batch and continuous flow at 10 bar H_2 and 150 °C, conditions were chosen to maximise hydrogen solubility[55] and promote ring-opening,[21,56] while minimising competing, undesired C–C bond cleavage.[57] Pure oxide supports were inactive for FALC conversion under batch and flow operation. Toluene was selected as a non-polar, inert solvent to minimise humin formation[58] and acetalisation, or competition with reactants for solid acid sites (and neutralisation of Lewis acidity), which are reported in protic solvents over acidic catalysts.[59–61] Lewis acidic Ru_3Sn_7/ZnO catalysts also exhibit higher selectivity to 1,5-PeD from furfural in non-alcoholic solvents.[62] Neither methylcyclohexane nor any hydrocarbon derivative of toluene was observed, consistent with our previous work on *m*-cresol hydrodeoxygenation (HDO) over Pt/ASA catalysts in toluene under more forcing conditions (200 °C and 20 bar H_2).[52] Note that downstream separation of the desired α,ω-diol products from toluene is amenable to energy-efficient liquid–liquid extraction by membrane filtration[63] wherein an organophilic pervaporation membrane (*e.g.* polydimethylsiloxane–polysulfone) permits a higher flux of toluene (less diffusion resistance).[64] In all experiments, carbon mass balances were between 94% and 99%, and carbon deposition (from elemental analysis) post-reaction ≤ 0.4 wt%, indicating minimal humin formation.

In batch, FALC conversion was proportional to support acid loading (Table 1), being <5% in 1 h for silica-supported Pt catalysts (Fig. S8†), *versus* 18%, 32%, and 73% for Pt/Al_2O_3, Pt/Al-SBA15(15), and Pt/ASA(61), respectively (Fig. 2a). Only the Pt/ASA(61) catalyst achieved complete conversion in 3 h, with no evidence of deactivation, whereas all other catalysts exhibited a sharp decrease in reaction kinetics after 1–2 h reaction despite a high concentration of the alcohol reactant. All catalysts evidenced reductive decarbonylation to furan, ring hydrogenation to THFA, and ring-opening to 1,5-PeD and 1,2-PeD, alongside trace MTHF from FALC hydrodeoxygenation. The desired 1,5-PeD was the dominant product in all cases, with yields proportional to acid loading (Fig. 2b) increasing from ~1% over Pt/SBA-15 to 41% for Pt/ASA(61) after 1 h reaction (Fig. 2b). Product selectivity was stable over the most acidic Pt/ASA(61) (Fig. 2c) and Pt/Al-SBA-15(15) however the remaining catalysts showed an increase in decarbonylation/dehydration at the expense of ring-opening during the first hour of reaction (Fig. S8†). Nevertheless, all three Al-containing catalysts exhibited similar selectivity to all products (1,5-PeD ~ 50%) at 10% iso-conversion of FALC, indicating a common active site and reaction mechanism. The optimum FALC conversion and 1,5-PeD yield for Pt/ASA(61) are comparable or superior to literature reports (Table S2†) and attained using a lower H_2 pressure (10 bar for this work *versus* ≥20 bar).

Under continuous flow, the influence of liquid residence time τ (defined as bed volume/flow rate) on FALC conversion and product selectivity was investigated over the Pt catalysts to identify the optimum support and flow rate for 1,5-PeD production. For all catalysts, minimal (<10%) conversion was observed at $\tau < 6$ min, with FALC conversion increasing in a sigmoidal fashion with residence time reaching a plateau at $\tau > 25$ min (Fig. 3a). However, as for batch hydrogenation, the magnitude of FALC conversion was sensitive to the support acidity, with a maximum single pass conversion of only ~10% for silica-supported Pt catalysts, and 73–98% for Pt nanoparticles on Al-containing strongly acidic supports. A residence time of 18 min (for which conversion and τ were linearly proportional and hence kinetics free from mass-transport limitations) and 1 h time-on-stream (to achieve steady state) were chosen to compare product selectivity. As observed in batch operation, all catalysts were active for reductive ring-opening to 1,5-PeD and 1,2-PeD as major pathways, in

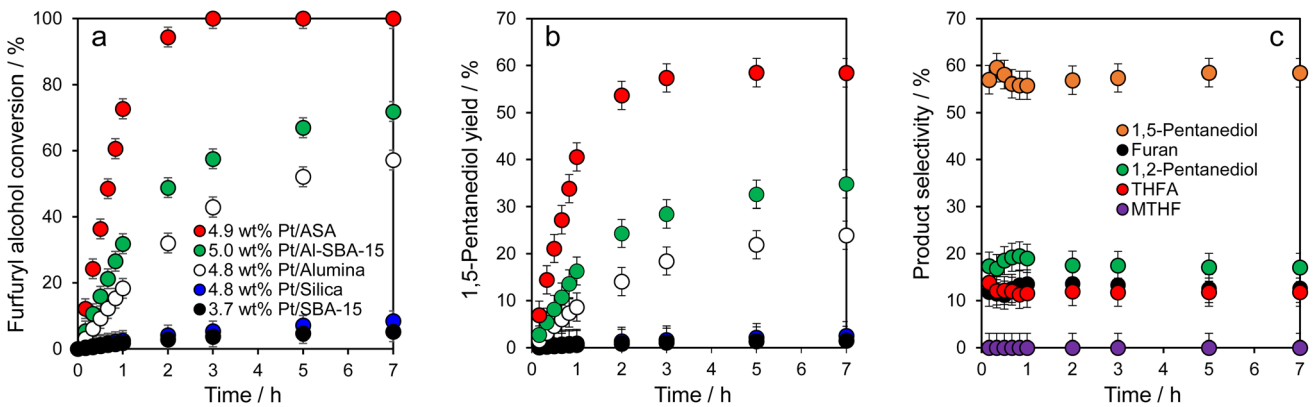

Fig. 2 (a) Furfuryl alcohol conversion and (b) 1,5-PeD yield over all Pt catalysts, and (c) product selectivity over Pt/ASA(61) during batchwise hydrogenation. Reaction conditions: 100 mg catalyst, 150 °C, 10 bar H_2, 10.86 mmol FALC in 50 cm^3 toluene, 800 rpm.

Open Access Article. Published on 15 July 2025. Downloaded on 2/3/2026 9:11:44 PM.
This article is licensed under a Creative Commons Attribution-NonCommercial 3.0 Unported Licence.

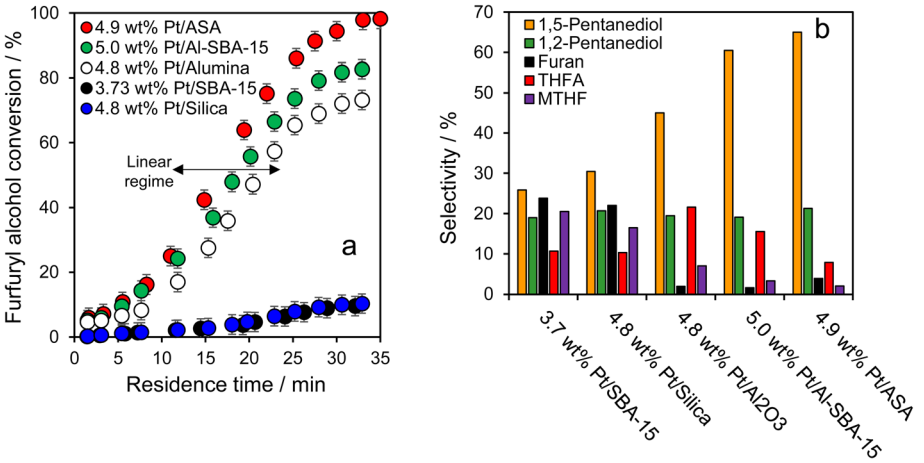

Fig. 3 (a) Influence of residence time on FALC conversion, and product selectivity over (b) all Pt catalysts, during continuous flow hydrogenation for $\tau = 18$ min (0.17 cm^3 min^{-1}). Reaction conditions: 100 mg catalyst, 10 bar H_2 and 150 °C, 0.22 M FALC in toluene, liquid flow rate 0.08 cm^3 min^{-1} to 2.06 cm^3 min^{-1}, 40 cm^3 min^{-1} H_2 through a GAM II hydrogen addition module.

competition with decarbonylation to furan, ring hydrogenation to THFA, and hydrodeoxygenation to MTHF. Selectivity to 1,5-PeD was likewise proportional to the support acidity (Fig. 3b), increasing from 26% over Pt/SBA-15 to 65% over Pt/ASA(61). THFA and diol production were uncorrelated, suggesting that the former is not a reaction intermediate in ring-opening under these conditions. This observation is consistent with the literature, for which the only report of Pt-catalysed THFA ring-opening required Brønsted acidic WO_x sites for C–O hydrogenolysis *via* an oxocarbenium ion and achieved a very low 1,5-PeD yield < 4% (albeit at only 90 °C). Selectivity to 1,5-PeD was directly proportional to the acid loading (Fig. S9†) across all catalysts, again consistent with a common active site and reaction mechanism. Comparison of Al_2O_3, Al-SBA-15, and ASA and silica-supported catalysts at low 10% iso-conversion confirmed that Pt/ASA(61) exhibited the highest selectivity to 1,5-PeD (Fig. S10†), and hence the importance of proximity between metal and acid sites to maximise the rates of both hydrogenation and ring-opening. These observations are consistent with previous studies of *m*-cresol and anisole HDO wherein proximate Pt nanoparticles and Brønsted acid sites increased reactant conversion and kinetics.[52,54] Neither catalyst deactivation nor significant changes in product selectivity were observed for any catalyst at the optimal $\tau = 18$ min over 7 h time-on-stream (Fig. S11†), consistent with negligible Pt or Al leaching (by ICP-AES) and only trace surface carbon in the post-reaction catalysts (by elemental analysis, Fig. S12†).

The impact of support acidity on catalyst activity for FALC conversion in batch and flow hydrogenation is summarised in Fig. 4a. Weakly acidic silicas were ineffective in promoting any Pt catalysis at 150 °C and 10 bar H_2. Introduction of support acidity through pure alumina or aluminosilicate phases activated FALC in batch and flow, provided metal and acid functions were in proximity; control experiments with physical mixtures of Pt/SiO_2 and either Al_2O_3, Al-SBA-15(15), or ASA(61) showed no metal–acid synergy (Fig. S13†). 1,5-PeD formation therefore likely proceeds *via* a short-lived surface intermediate, stabilised by the concerted action of Pt nanoparticles in close proximity to Brønsted acid sites. This metal–acid synergy is akin to that recently reported for anisole[54] and *m*-cresol[52] hydrogenation over aluminosilicate-supported Pt nanoparticles (in toluene) and that reported between Cu^+ and Brønsted acid sites (in ethanol).[27] To our knowledge, the mechanism of furfuryl alcohol ring-opening has only been studied by Dai *et al.*,[27] whose combined experimental and DFT approach indicated that either the C2 or C5 atoms in the furan ring are first protonated by Brønsted acid sites to form corresponding carbocations. The C5 carbocation intermediate is less stable than its C2 counterpart, and hence cleavage of the C2–O bond is faster than that of the C5–O bond, favouring the formation of the 1,5-PeD precursor accompanied by deprotonation to regenerate the Brønsted acid site. Finally, the 1,5-PeD precursor undergoes metal-catalysed hydrogenation to the 1,5-pentanediol product. Consequently, 1,5-PeD productivity increased dramatically from only 7 mmol g_{Pt}^{-1} h^{-1} over Pt/silicas to 186 mmol g_{Pt}^{-1} h^{-1} over Pt/ASA(61) (Fig. 4b). As for batch operation, the optimum FALC steady-state conversion and 1,5-PeD yield for Pt/ASA(61) are comparable or superior to literature reports (Table S3†) despite our lower H_2 pressure. Although neither Pt or Al leaching nor significant carbon accumulation was observed for any spent catalysts, and stable furfuryl alcohol conversion and product selectivity were observed over 7 h reaction, in future it would be valuable to determine the acid properties post-reaction; such measurements are hindered by the presence of quartz chips as an inert diluent in the packed bed. Note that a different reaction mechanism is proposed over PtCoCe ternary oxide catalysts, wherein the reducible metal oxides confer Lewis acidity (associated with oxygen vacancies) that is proposed to mediate protonation of the C2–O bond.[65] Brønsted acidity may also be less important in C–O bond cleavage in linear saturated ethers, *e.g.* dicyclohexyl ether, wherein Lewis acid sites can catalyse the hydrolysis of ether bonds.[66]

Considering the reaction pathways for FALC, furan and MTHF are only significant products over the weakly acidic silica

© 2025 The Author(s). Published by the Royal Society of Chemistry

Open Access Article. Published on 15 July 2025. Downloaded on 2/3/2026 9:11:44 PM.
This article is licensed under a Creative Commons Attribution-NonCommercial 3.0 Unported Licence.

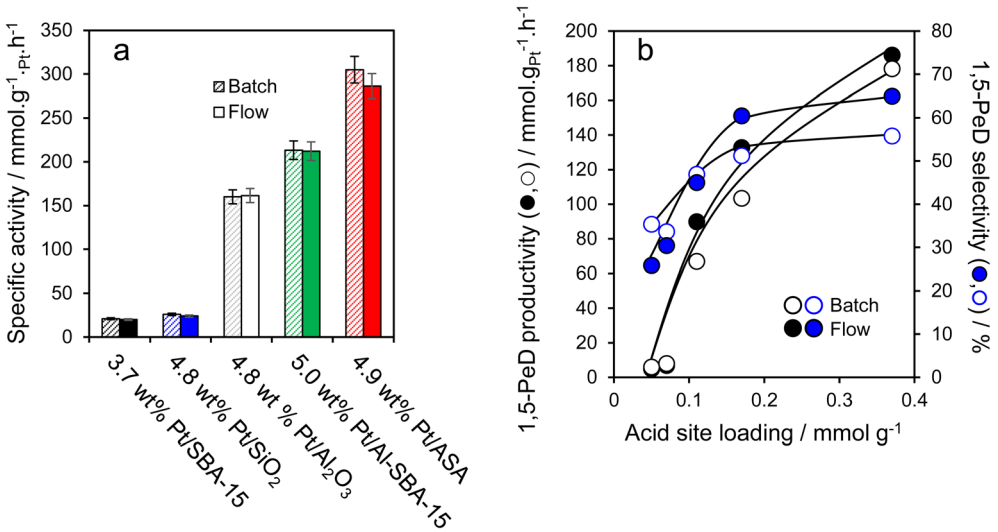

Fig. 4 (a) Specific activity for FALC conversion over different Pt/catalysts in batch and flow hydrogenation, and (b) 1,5-pentanediol productivity and selectivity (batch and flow) after 1 h reaction as a function of acid site loading. Reaction conditions: 100 mg catalyst, 10 bar H_2 and 150 °C; and 10.86 mmol FALC in 50 cm^3 toluene, 800 rpm in batch; or 0.22 M furfuryl alcohol in toluene, $\tau = 18$ min (liquid flow rate ~ 0.17 cm^3 min^{-1}), 40 cm^3 min^{-1} H_2 in flow.

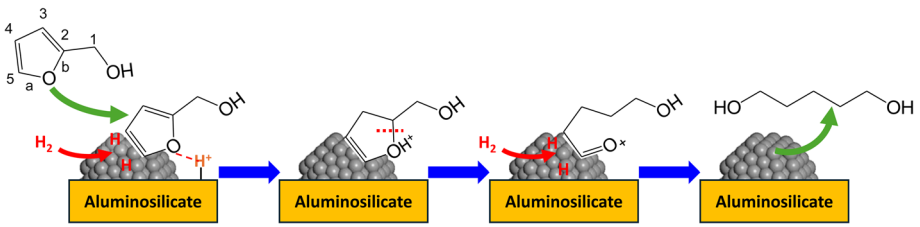

Fig. 5 Proposed reaction pathway for 1,5-PeD formation from FALC over Pt/acid supports.

supports (Fig. 3b), for which platinum chemistry is expected to dominate. This is consistent with temperature-programmed reaction studies of furfural adsorbed over a Pt(111) single crystal surface which was effective for decarbonylation to furan (at low surface coverages).[56] Pre-adsorbed hydrogen promotes furfural hydrogenation to FALC and the latter's subsequent hydrodeoxygenation to methyl furan. Ring-opening of FALC over Pt nanoparticles alone can therefore be discounted. In contrast, DFT calculations suggest a low-temperature, acid-catalysed route to 1,5-PeD through a partially hydrogenated intermediate of FALC.[67] Bond energies for ether cleavage (C–O–C) in the 2,3- or 4,5-dihydrofurfuryl alcohol partial hydrogenation products of FALC are lower (1.455 eV and 1.378 eV, respectively) than their fully hydrogenated analogues (1.433 and 1.449 eV, respectively).[13] Building on our earlier mechanistic discussion, we therefore conclude that FALC adsorbed at the perimeter of Pt nanoparticles and acidic supports are activated for simultaneous ring hydrogenation and C–O–C protonation (by H adatoms generated over Pt metal sites), facilitating efficient C–O hydrogenolysis. Hydrogenation at the C2–C3 double bond is proposed to direct 1-5-PeD formation, *via* the aforementioned short-lived partially hydrogenated intermediates formed at the interface between Pt nanoparticles and Lewis/Brønsted acid sites (Fig. 5).[13] Alternatively, direct protonation of the CH_2OH can lead to spontaneous ring opening in furfural as proposed for Cu/MFI, but is less selective with other side reactions competing (*e.g.* Piancatelli rearrangement).[27]

Conclusions

The role of solid acidity in the Pt-catalysed hydrogenolysis of furfuryl alcohol (FALC) to 1,5-pentanediol (1,5-PeD) was studied for a family of silica and aluminosilicate supports. Siliceous supports, whether amorphous or structured (mesoporous SBA-15), possess a low concentration of acid sites and proved ineffective in promoting a common loading (~5 wt%) of Pt nanoparticles for FALC chemistry under batchwise and continuous flow operation at 150 °C and 10 bar H_2. Only traces (<5% each) of 1,5-PeD (and the corresponding 1,2-propanediol) were observed for Pt/SiO_2 and Pt/SBA-15, in competition with reductive decarbonylation to furan, hydrodeoxygenation to methyltetrahydrofuran, and ring hydrogenation to tetrahydrofurfuryl alcohol. In contrast, aluminosilicate supports possessing high loadings of Brønsted and Lewis acid sites and specific surface areas >270 m^2 g^{-1} promoted FALC activation over Pt nanoparticles, dramatically increasing both conversion

© 2025 The Author(s). Published by the Royal Society of Chemistry

Open Access Article. Published on 15 July 2025. Downloaded on 2/3/2026 9:11:44 PM. This article is licensed under a Creative Commons Attribution-NonCommercial 3.0 Unported Licence.

and selectivity to the desired 1,5-PeD product. The yield of 1,5-PeD was proportional to total acid site loading, suggesting that FALC ring opening was agnostic to the type of acid site or the support textural properties. Appropriate selection of the residence time enabled similar reaction kinetics for batch and flow hydrogenation of FALC. Maximum 1,5-PeD productivity (186 mmol g_{Pt}^{-1} h^{-1}) and selectivity (65%) were obtained for a 5 wt% Pt/ASA(61) catalyst and retained for 7 h reaction with negligible deactivation. Judicious selection of acidic supports to induce a strong metal–acid synergy offers a low-cost route to dramatically promote the selective hydrogenation of biomass-derived furanics, and one that is readily translated from conventional batch to scalable flow chemistry without loss of performance.

Data availability

Data supporting this article have been included as part of the ESI,† with original data available on request from the corresponding authors.

Author contributions

Lee J. Durndell; conceptualisation, resources, methodology, data curation, formal analysis, investigation, writing – original draft, writing – review and editing. Vannia C. dos Santos-Durndell; formal analysis, writing – original draft, writing – review and editing. Atal Shivhare; data curation, formal analysis. James A. Hunns; data curation, formal analysis. Karen Wilson; conceptualisation, resources, supervision, writing – review and editing. Adam F Lee; conceptualisation, resources, supervision, writing – review and editing.

Conflicts of interest

The authors declare that no known competing financial or personal interests may have influenced the work reported.

Acknowledgements

We thank the EPSRC (EP/K036548/1 and EP/K014706/1) and Australian Research Council (DP200100204, DP200100313, and LE210100100) for financial support. KW thanks the Royal Society for an Industry Fellowship. Support from the European Union Seventh Framework Programme (FP7/2007-2013) under grant agreement no. 604307 is also acknowledged. LJD thanks the RSC (R19-2791 and M19-1518) for financial support.

References

1 J. Melrose, R. Perroy and S. Careas, Working Paper No. ESA/P/WP.241, 2015.
2 P. Gerland, A. E. Raftery, H. Ševčíková, N. Li, D. Gu, T. Spoorenberg, L. Alkema, B. K. Fosdick, J. Chunn, N. Lalic, G. Bay, T. Buettner, G. K. Heilig and J. Wilmoth, *Science*, 2014, **346**, 234–237.
3 A. S. Mamman, J.-M. Lee, Y.-C. Kim, I. T. Hwang, N.-J. Park, Y. K. Hwang, J.-S. Chang and J.-S. Hwang, *Biofuel Bioprod. Biorefining*, 2008, **2**, 438–454.
4 R. Xing, W. Qi and G. W. Huber, *Energy Environ. Sci.*, 2011, **4**, 2193–2205.
5 G. W. Huber, S. Iborra and A. Corma, *Chem. Rev.*, 2006, **106**, 4044–4098.
6 J.-P. Lange, E. van der Heide, J. van Buijtenen and R. Price, *ChemSusChem*, 2012, **5**, 150–166.
7 B. Zhang, Y. Zhu, G. Ding, H. Zheng and Y. Li, *Green Chem.*, 2012, **14**, 3402–3409.
8 H. Liu, Z. Huang, F. Zhao, F. Cui, X. Li, C. Xia and J. Chen, *Catal. Sci. Technol.*, 2016, **6**, 668–671.
9 G. M. King, S. Iqbal, P. J. Miedziak, G. L. Brett, S. A. Kondrat, B. R. Yeo, X. Liu, J. K. Edwards, D. J. Morgan, D. K. Knight and G. J. Hutchings, *ChemCatChem*, 2015, **7**, 2122–2129.
10 F. Dong, Y. Zhu, G. Ding, J. Cui, X. Li and Y. Li, *ChemSusChem*, 2015, **8**, 1534–1537.
11 V. Vorotnikov, G. Mpourmpakis and D. G. Vlachos, *ACS Catal.*, 2012, **2**, 2496–2504.
12 D. K. Mishra, S. Kumar and R. S. Shukla, in *Biomass, Biofuels, Biochemicals*, ed. S. Saravanamurugan, A. Pandey, H. Li and A. Riisager, Elsevier, 2020, DOI: 10.1016/B978-0-444-64307-0.00012-3, pp. 323–353.
13 K. Tomishige, M. Honda, H. Sugimoto, L. Liu, M. Yabushita and Y. Nakagawa, *Carbon Neutrality*, 2024, **3**, 17.
14 K. Huang, W. Won, K. J. Barnett, Z. J. Brentzel, D. M. Alonso, G. W. Huber, J. A. Dumesic and C. T. Maravelias, *Appl. Energy*, 2018, **213**, 585–594.
15 Z. J. Brentzel, K. J. Barnett, K. Huang, C. T. Maravelias, J. A. Dumesic and G. W. Huber, *ChemSusChem*, 2017, **10**, 1351–1355.
16 H. Adkins and R. Connor, *US Pat.*, US2094975A, 1937.
17 W. Xu, H. Wang, X. Liu, J. Ren, Y. Wang and G. Lu, *Chem. Commun.*, 2011, **47**, 3924–3926.
18 S. Liu, Y. Amada, M. Tamura, Y. Nakagawa and K. Tomishige, *Green Chem.*, 2014, **16**, 617–626.
19 M. Hronec, K. Fulajtárová and T. Soták, *J. Ind. Eng. Chem.*, 2014, **20**, 650–655.
20 M. Pirmoradi, N. Janulaitis, R. J. Gulotty Jr and J. R. Kastner, *ACS Omega*, 2020, **5**, 7836–7849.
21 Y. Nakagawa and K. Tomishige, *Catal. Today*, 2012, **195**, 136–143.
22 L. J. Durndell, G. Zou, W. Shangguan, A. F. Lee and K. Wilson, *ChemCatChem*, 2019, **11**, 3927–3932.
23 J. Peng, D. Zhang, Y. Wu, H. Wang, X. Tian and M. Ding, *Fuel*, 2023, **332**, 126261.
24 J. Tan, Y. Su, X. Hai, L. Huang, J. Cui, Y. Zhu, Y. Wang and Y. Zhao, *Mol. Catal.*, 2022, **526**, 112391.
25 Y. Shao, M. Guo, J. Wang, K. Sun, L. Zhang, S. Zhang, G. Hu, L. Xu, X. Yuan and X. Hu, *Ind. Eng. Chem. Res.*, 2021, **60**, 10393–10406.
26 D. Dai, Y. Shi, C. Feng, D. Liu and Y. Liu, *Microporous Mesoporous Mater.*, 2023, **351**, 112484.
27 D. Dai, C. Feng, M. Wang, Q. Du, D. Liu, Y. Pan and Y. Liu, *Catal. Sci. Technol.*, 2022, **12**, 5879–5890.

© 2025 The Author(s). Published by the Royal Society of Chemistry

Open Access Article. Published on 15 July 2025. Downloaded on 2/3/2026 9:11:44 PM. This article is licensed under a Creative Commons Attribution-NonCommercial 3.0 Unported Licence.

28 A. S. Nimbalkar, K.-R. Oh, D.-Y. Hong, B. G. Park, M. Lee, D. W. Hwang, A. Awad, P. P. Upare, S. J. Han and Y. K. Hwang, *Green Chem.*, 2024, **26**, 11164–11176.
29 Y. Yang, Q. Liu and Z. Liu, *Catalysts*, 2024, **14**, 223.
30 V. V. Kumar, G. Naresh, M. Sudhakar, J. Tardio, S. K. Bhargava and A. Venugopal, *Appl. Catal., A*, 2015, **505**, 217–223.
31 L. Bui, H. Luo, W. R. Gunther and Y. Román-Leshkov, *Angew. Chem., Int. Ed.*, 2013, **52**, 8022–8025.
32 H. Li, S. Zhang and H. Luo, *Mater. Lett.*, 2004, **58**, 2741–2746.
33 C. M. A. Parlett, L. J. Durndell, A. Machado, G. Cibin, D. W. Bruce, N. S. Hondow, K. Wilson and A. F. Lee, *Catal. Today*, 2014, **229**, 46–55.
34 S. H. Krishna, R. S. Assary, Q. A. Rashke, Z. R. Schmidt, L. A. Curtiss, J. A. Dumesic and G. W. Huber, *ACS Catal.*, 2018, **8**, 3743–3753.
35 L. J. Durndell, K. Wilson and A. F. Lee, *RSC Adv.*, 2015, **5**, 80022–80026.
36 E. Gross, J. H.-C. Liu, F. D. Toste and G. A. Somorjai, *Nat. Chem.*, 2012, **4**, 947–952.
37 M. O'Brien, N. Taylor, A. Polyzos, I. R. Baxendale and S. V. Ley, *Chem. Sci.*, 2011, **2**, 1250–1257.
38 D. Zhao, J. Feng, Q. Huo, N. Melosh, G. H. Fredrickson, B. F. Chmelka and G. D. Stucky, *Science*, 1998, **279**, 548–552.
39 K. B. Baharudin, M. Arumugam, J. Hunns, A. F. Lee, E. Mayes, Y. H. Taufiq-Yap, K. Wilson and D. Derawi, *Catal. Sci. Technol.*, 2019, **9**, 6673–6680.
40 L. J. Durndell, C. M. A. Parlett, N. S. Hondow, M. A. Isaacs, K. Wilson and A. F. Lee, *Sci. Rep.*, 2015, **5**, 9425.
41 L. J. Durndell, C. Cucuzzella, C. M. A. Parlett, M. A. Isaacs, K. Wilson and A. F. Lee, *Catal. Today*, 2019, **333**, 161–168.
42 R. Chen, Z. Chen, B. Ma, X. Hao, N. Kapur, J. Hyun, K. Cho and B. Shan, *Comput. Theor. Chem.*, 2012, **987**, 77–83.
43 X. Liu, *J. Phys. Chem. C*, 2008, **112**, 5066–5073.
44 Y. Matsunaga, H. Yamazaki, T. Yokoi, T. Tatsumi and J. N. Kondo, *J. Phys. Chem. C*, 2013, **117**, 14043–14050.
45 W. H. Dawson, S. W. Kaiser, P. D. Ellis and R. R. Inners, *J. Phys. Chem.*, 1982, **86**, 867–868.
46 W. Hua, Y. Yue and Z. Gao, *J. Mol. Catal. A: Chem.*, 2001, **170**, 195–202.
47 L. Chmielarz, P. Kuśtrowski, M. Drozdek, M. Rutkowska, R. Dziembaj, M. Michalik, P. Cool and E. F. Vansant, *J. Porous Mater.*, 2011, **18**, 483–491.
48 H. Y. Luo, J. D. Lewis and Y. Román-Leshkov, *Annu. Rev. Chem. Biomol. Eng.*, 2016, **7**, 663–692.
49 W. Sun, H. Li, X. Wang and A. Liu, *Front. Chem.*, 2022, **10**, 2022.
50 P. Sudarsanam, N. K. Gupta, B. Mallesham, N. Singh, P. N. Kalbande, B. M. Reddy and B. F. Sels, *ACS Catal.*, 2021, **11**, 13603–13648.
51 A. I. M. Rabee, L. J. Durndell, N. E. Fouad, L. Frattini, M. A. Isaacs, A. F. Lee, G. A. H. Mekhemer, V. C. d. Santos, K. Wilson and M. I. Zaki, *Mol. Catal.*, 2018, **458**, 206–212.
52 J. A. Hunns, L. J. Durndell, X. Zhang, M. Konarova, A. F. Lee and K. Wilson, *ACS Catal.*, 2024, **14**, 7052–7061.
53 K. B. Baharudin, Y. H. Taufiq-Yap, J. Hunns, M. Isaacs, K. Wilson and D. Derawi, *Microporous Mesoporous Mater.*, 2019, **276**, 13–22.
54 A. Shivhare, J. A. Hunns, L. J. Durndell, C. M. A. Parlett, M. A. Isaacs, A. F. Lee and K. Wilson, *ChemSusChem*, 2020, **13**, 4945–4953.
55 J.-Z. Yin and C.-S. Tan, *Fluid Phase Equilib.*, 2006, **242**, 111–117.
56 M. J. Taylor, L. Jiang, J. Reichert, A. C. Papageorgiou, S. K. Beaumont, K. Wilson, A. F. Lee, J. V. Barth and G. Kyriakou, *J. Phys. Chem. C*, 2017, **121**, 8490–8497.
57 S. Sitthisa, W. An and D. E. Resasco, *J. Catal.*, 2011, **284**, 90–101.
58 S. Liu, Y. Zhu, Y. Liao, H. Wang, Q. Liu, L. Ma and C. Wang, *Appl. Energy Combust. Sci.*, 2022, **10**, 100062.
59 N. Shi, Q. Liu, H. Cen, R. Ju, X. He and L. Ma, *Biomass Convers. Biorefin.*, 2020, **10**, 277–287.
60 M. J. Taylor, L. J. Durndell, M. A. Isaacs, C. M. A. Parlett, K. Wilson, A. F. Lee and G. Kyriakou, *Appl. Catal., B*, 2016, **180**, 580–585.
61 D. S. S. Jorqueira, L. F. de Lima, S. F. Moya, L. Vilcocq, D. Richard, M. A. Fraga and R. S. Suppino, *Appl. Catal., A*, 2023, **665**, 119360.
62 P. P. Upare, Y. Kim, K.-R. Oh, S. J. Han, S. K. Kim, D.-Y. Hong, M. Lee, P. Manjunathan, D. W. Hwang and Y. K. Hwang, *ACS Sustain. Chem. Eng.*, 2021, **9**, 17242–17253.
63 S. Divakar, M. Padaki and R. G. Balakrishna, *ACS Omega*, 2022, **7**, 44495–44506.
64 S. Chaudhari, H. Shin, S. Choi, K. Cho, M. Shon, S. Nam and Y. Park, *RSC Adv.*, 2021, **11**, 9274–9284.
65 Y. Li, J. Zhang, W. Zhang, C. Zhou, J. Huang, Z. Su, Z. Qiao, X. Qin, P. Xiong and F.-S. Xiao, *ACS Catal.*, 2025, **15**, 7731–7740.
66 G. F. Leal, S. Lima, I. Graça, H. Carrer, D. H. Barrett, E. Teixeira-Neto, A. A. S. Curvelo, C. B. Rodella and R. Rinaldi, *iScience*, 2019, **15**, 467–488.
67 X. Wang, Y. Weng, X. Zhao, X. Xue, S. Meng, Z. Wang, W. Zhang, P. Duan, Q. Sun and Y. Zhang, *Ind. Eng. Chem. Res.*, 2020, **59**, 17210–17217.

© 2025 The Author(s). Published by the Royal Society of Chemistry